Grenze International Journal of Engineering and Technology, Jan Issue

Performance Evaluation of a Sliding Mode Controlled DC to DC Converter for EV Charging System

Annepu BalaKrishna[1], Abhishek Pintu.k[2], Vamsi Krishna.P[3] and Prof .Rama Sudha.K[4]
[1-4]Andhra University/Electrical Engineering Department, Visakhapatnam, India
Email: annepubalakrishna12221@gmail.com, {abhishek.kollabathula, askvamsi3}@ gmail.com, prof.kramasudha@andhrauniversity.edu.in

***Abstract*— Due to environmental concerns, electric vehicles (EVs) are becoming more and more common in automobiles. Since electrical vehicles rely on rechargeable batteries to manage their power supply, therefore, it's important to have a reliable, efficient, and affordable battery charger that can consistently deliver the required output for the specific EV's battery. A DC-DC converter with a pulse width modulation (PWM) based Sliding-Mode Voltage controller is presented in this paper to help reduce charging time by achieving the required output voltage, high current density, and negligible overshoot for the specified lithium-ion battery system. Both ideal and non-ideal conditions are used to analyse the proposed converter. The performance of dc and ac side inductors has been designed and analysed to ensure their efficiency and affordability. According to the findings, the proposed converter is able to maintain a power factor of approximately 90% with less total harmonic distortion both of which are ideal for the high-current density load.**

***Index Terms*— Buck, lithium-ion battery charger, electric vehicle battery charger, ac-dc converter, MOSFET, Pulse Width Modulation (PWM), Sliding-Mode (SM)**

I. INTRODUCTION

The rechargeable battery is one of the crucial and complex systems that provides electricity to drive electric vehicles (EVs). Therefore, having an effective, affordable, and efficient battery charger is essential for EVs. To completely meet the requirement, an AC-DC converter is required [1],[2],[3][4]. An AC-DC converter can be isolated or non-isolated. In this paper conventional diode based AC -DC converter is used along with proper designed LCL filter in order to reduce unwanted harmonic distortion and to increase overall power factor of system [5],[6],[7][8].
Afterward, depending on the state of the lithium-ion battery, the voltage may need to be adjusted. A closed-loop DC-DC converter can be utilized to do this operation. The life cycle of the entire system may be shortened by the considerable power loss that the traditional closed-loop DC-DC converter dissipates in the active switches [9],[10]. Conduction, switching, and leakage power losses cause the largest power loss in typical closed-loop DC-DC converters. Additionally, the output voltage and current do exhibit overshoot, which may be harming the lithium-ion battery[11],[12].
To overcome, a Pulse Width Modulation (PWM) based Sliding-Mode Voltage controller is used. This controller

Grenze ID: 01.GIJET.10.1.18_1

aids in reducing conduction power loss, switching power loss, and leakage power loss in addition to the overshoot at the output voltage and current. Additionally, the present prosecution has been enhanced [13],[14]. This suggests that the overall power loss will be decreased without compromising the switching frequency, which helps to keep the size of passive components constant.
This study presents a reliable, cost-effective, and efficient AC-DC converter for lithium-ion battery charging in electric vehicles. Distinct situations are used to study the converter in detail.

II. Helpful Hints

A. Proposed system

The proposed system is illustrated in Fig .1. The load is supplied with electricity by the single-phase ac source. The LCL network has been allocated near the ac source for filtering reasons. The diodes D5, D6 , D7and D8 aid in controlling the ac flow to the connected primary side. The rippled waves in the DC are lessened by the RC3, C3. Afterwards, the two MOSFETs M1, M2 and then assist in adjusting the dc output voltage in response to the load. The remaining diodes, D1, D2, D3, and D4, aid in preserving the dc flow. Components like L1, L2, and C1 are responsible for storing and filtering purposes. The two fuses F1 and F2 are assigned for protection. Eventually, the Lithium-Ion battery (48V 100Ah) was used as a load.

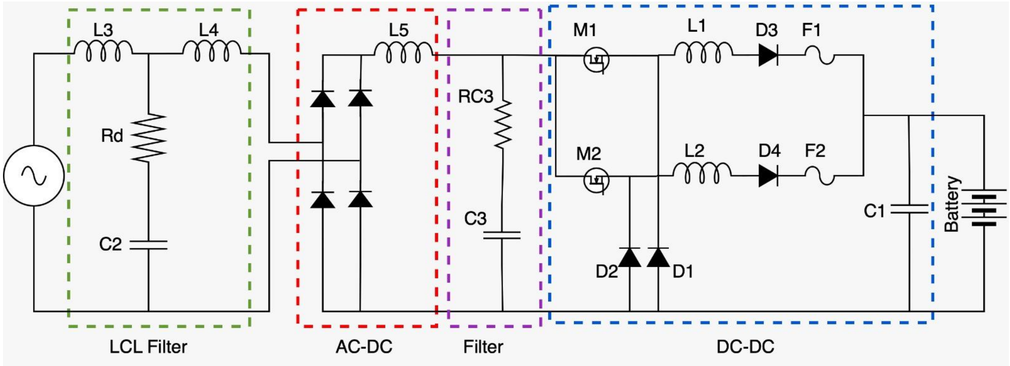

Fig.1 proposed system

B. Design and analysis of LCL filter

The grid current can be estimated based on equation 1.

$$I_{grid} = \frac{\sqrt{2} \times P_{load}}{V_{ac}} A \tag{1}$$

The required inductance can be computed using equation 2.

$$L = \frac{X_l}{2 \times \pi \times f_{ac}} H \tag{2}$$

where, x L = Inductor reactance = 2πf L
The L3 and L4 will be half of the inductance that has been calculated.
The ac side capacitance can be calculated as

$$C_2 = \frac{1\% \times P_{load}}{2 \times \pi \times f_{ac} \times V_{ac}^2} F \tag{3}$$

The resonant frequency can be computed as

$$F_r = \frac{1}{2 \times \pi \times \sqrt{\frac{L_3 \times L_4}{L_3 + L_4} \times C_2}} HZ \tag{4}$$

The damping resistance can be calculated as

$$R_d = \frac{1}{6 \times \pi \times F_r \times C_2} \, ohm \quad (5)$$

Where f_{ac} = Grid frequency, P_{load} = Filter load power. The designed filter frequency response can be analysed based on the transfer function and given herewith.

$$SYS(s) = \frac{R_d \times C_2 + 1}{L_3 \times L_4 \times C_2 s^3 + (L_3 + L_4) \times R_d \times C_2 s^2 + (L_3 + L_4) s} \quad (6)$$

After manipulating the above equations, the bode plot has been computed and depicted in Figure 2. The Figure implicates the consequences of the designed filter frequency response and the stability. After adding the damping resistor, the overall response smooth and minimizes the spike that is associated with the system besides when the damping resistor was not concerned spikes do take place. Thus we can conclude from bode plots , that the designed filter exhibits more stability while the damping resistor is integrated .

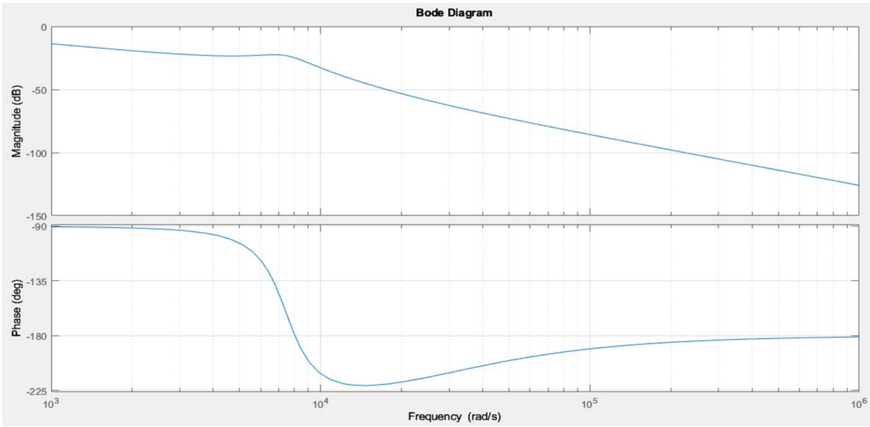

(a)

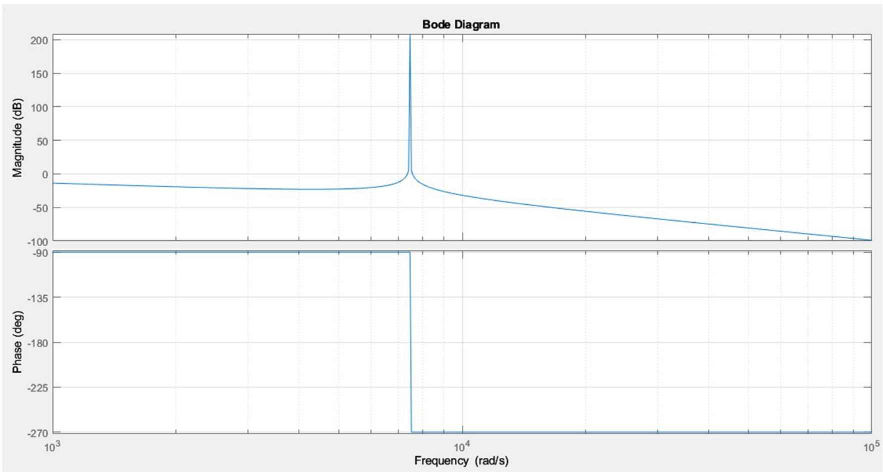

(b)

Fig 2. Bode plot of the designed LCL filter (a) with effect of R_d (b) without R_d

C. Steady state analysis of the proposed DC-DC system

a. *Ideal condition*

For the sake of this study, all the components are considered perfect. In addition, fixed switching frequency and duty cycle have been examined. A continuous open-loop analysis of the system is being conducted. The four modes of the suggested DC-DC converter have been explored here.

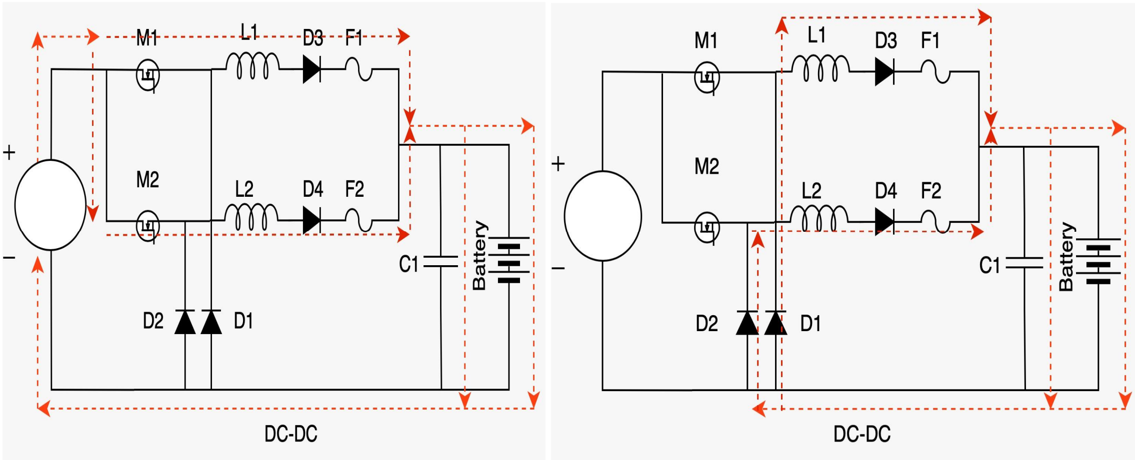

Mode One Mode Two

Fig.3 Working modes of the proposed DC-DC converter: (a) Mode One (b) Mode Two

1. Mode one

The converter has performed an analysis at the time 0 t DTs. MOSFETs one and two are now operating in conduction mode, whereas MOSFETs three and four as well as diodes one and two are operating in non-conduction mode. As seen in Figure 2(a), the input source is now linked to the left side of inductors one and two. In this approach, the crucial equations are.

$$V_{L1} = V_g - V_0 \tag{7}$$

$$V_{L2} = V_g - V_0 \tag{8}$$

$$\frac{d_{iL1}}{dt} = \frac{V_g - V_0}{L_1} \tag{9}$$

$$\frac{d_{iL2}}{dt} = \frac{V_g - V_0}{L_2} \tag{10}$$

$$i_{C1} = I_{L12} - I_0 \tag{11}$$

2. Mode two

Now that the converter has been examined during the DTs to Ts timeframe. Four MOSFETs are currently operating in non-conduction mode. The first and second diodes are now conducting. Inductors one and two's left sides are now connected to the ground, and the circuit is now shown in Figure 2(b). In this approach, the key equations are.

$$V_{L1} = -V_0 \tag{12}$$

$$V_{L2} = -V_0 \tag{13}$$

$$\frac{d_{iL1}}{dt} = \frac{-V_0}{L_1} \tag{14}$$

$$\frac{d_{iL2}}{dt} = \frac{-V_0}{L_2} \tag{15}$$

$$i_{C1} = I_{L12} - I_0 \quad (16)$$

b. Non Ideal Conditions

For the sake of this investigation, the MOSFET has been chosen with the assumption that all of the components are not perfect. The system has been examined in continuous conduction mode with the frequency and duty cycle being presumptively constant. The preceding section described the two modes of the proposed DC-DC system.

1. Mode one

The important equations of this mode are.

$$V_{L1} = V_g - V_{M1} - I_{RL1}R_{M1} - I_{RL1}R_{L1} - V_{D3} - I_{RL1}R_{D3} - I_{RL1}R_{F1} - V_0 \quad (17)$$

$$V_{L2} = V_g - V_{M2} - I_{RL2}R_{M2} - I_{RL2}R_{L2} - V_{D4} - I_{RL2}R_{D4} - I_{RL2}R_{F2} - V_0 \quad (18)$$

$$\frac{d_{iL1}}{dt} = \frac{(V_g - V_{M1} - I_{RL1}R_{M1} - I_{RL1}R_{L1} - V_{D3} - I_{RL1}R_{D3} - I_{RL1}R_{F1} - V_0)}{L1} \quad (19)$$

$$\frac{d_{iL2}}{dt} = \frac{\left(V_g - V_{M2} - I_{RL2}R_{M2} - I_{RL2}R_{L2} - V_{D4} - I_{RL2}R_{D4} - I_{RL2}R_{F2} - V_0\right)}{L_2} \quad (20)$$

$$i_{C1} = I_{L12} - I_0 \quad (21)$$

2. Mode two

The important equations of this mode are.

$$V_{L1} = -I_{RL1}R_{L1} - V_{D3} - I_{RL1}R_{D3} - I_{RL1}R_{F1} - V_0 - I_{RL1}R_{D1} - V_{D1} \quad (22)$$

$$V_{L2} = -I_{RL2}R_{L2} - V_{D4} - I_{RL2}R_{D4} - I_{RL2}R_{F2} - V_0 - I_{RL2}R_{D2} - V_{D2} \quad (23)$$

$$\frac{d_{iL1}}{dt} = \frac{(-I_{RL1}R_{L1} - V_{D3} - I_{RL1}R_{D3} - I_{RL1}R_{F1} - V_0 - I_{RL1}R_{D1} - V_{D1})}{L1} \quad (24)$$

$$\frac{d_{iL2}}{dt} = \frac{(-I_{RL2}R_{L2} - V_{D4} - I_{RL2}R_{D4} - I_{RL2}R_{F2} - V_0 - I_{RL2}R_{D2} - V_{D2})}{L_2} \quad (25)$$

$$i_{C1} = I_{L12} - I_0 \quad (26)$$

At 0 < t < Ts the dc conversion ratio for L1 and L2 would be

$$L_1 = G_1 = D_{on} \times \left(\frac{2 \times \left(1 - \frac{V_{M1}}{V_g} - \frac{V_{D3}}{DV_g} - \frac{D_{off}V_{D1}}{DV_g}\right)}{\frac{DR_{M1} + R_{L1} + R_{D3} + R_{F1} + 2R + D_{off}R_{D1}}{R}} \right) \quad (27)$$

$$L_2 = G_2 = D_{on} \times \left(\frac{2 \times \left(1 - \frac{V_{M2}}{V_g} - \frac{V_{D4}}{DV_g} - \frac{D_{off}V_{D2}}{DV_g}\right)}{\frac{DR_{M2} + R_{L2} + R_{D4} + R_{F2} + 2R + D_{off}R_{D2}}{R}} \right) \quad (28)$$

D. Design of proposed Sliding-Mode Voltage Controller

SM (SLIDING-MODE) controllers are renowned for their dependability and stability. In order to achieve the necessary steady-state functioning, SM controllers should ideally operate at infinite, variable, and self-oscillating switching frequencies that allow the controlled variables to follow a certain reference route. However, the viability of using SM controllers in power converters is hampered by the fluctuating and high switching frequency. The controller's modelling includes the state-space averaging method. By doing this, the implementation of SM controllers may directly benefit from PWM duty cycle control. .

So, in this paper, we provide a unified approach to the design of PWM-based SM voltage controllers for fundamental dc-dc buck converter based on the work of [13]. Similar to [13], our goal is to give straightforward, immediately implementable control equations for the PWM-based SM voltage controller.

Creating a state-space description of the converter model in terms of the required control variables (such as voltage and/or current, etc.) is the first step in designing an SM controller. This research focuses on the use of SM control for converters that operate in CCM. It incorporates an extra voltage error integral term into the control computation, unlike the majority of other previously suggested SM voltage controllers, in order to lower the steady-state dc error of the actual SM controlled system.

fig. 4 shows the schematic diagrams of the PID SMVC dc–dc converters to be discussed in this paper . Here, C , L, and r_l denote the capacitance, inductance, and instantaneous load resistance of the converters respectively; i_c ,i_L and i_T denote the instantaneous capacitor, inductor, and load currents, respectively ;V_{ref} , v_i and v_0 denote the reference, instantaneous input, and instantaneous output voltages, respectively; β denotes the feedback network ratio; and $u = 0$ or1 is the switching state of power switch .

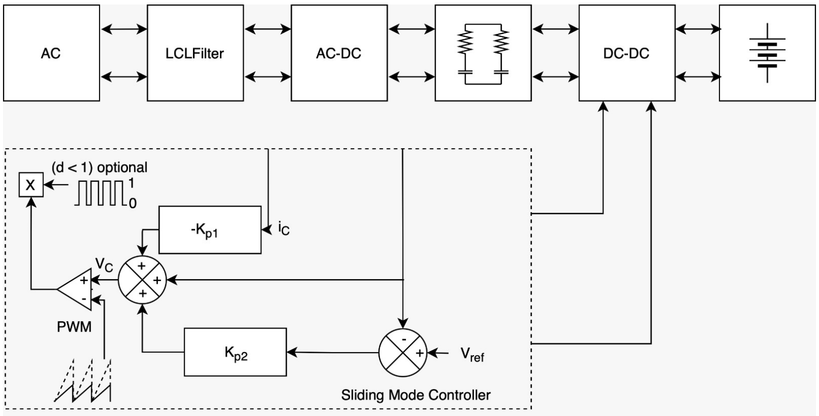

Fig .4 Schematic diagram of the PWM based SMVC buck converter.

The control equations required for the implementation of the respective buck converter are
The instantaneous state variable's trajectory is described as

$$S = \lambda_1 x_1 + \lambda_2 x_2 + \lambda_3 x_3$$

Where $\lambda_1, \lambda_2, and \lambda_3$ representing the control parameters termed as sliding coefficients.

Next, we look at how the converters' SM control operation's existence conditions are determined. The local reachability criterion is necessary to guarantee the presence of SM operation.

$$\lim_{s \to 0} S.\dot{S} < 0$$

For buck converter simplified existence condition is

$$0 < -\beta L_1 \left(\frac{\lambda_1}{\lambda_2} - \frac{1}{r_L C_1}\right) i_c + L_1 C_1 \frac{\lambda_3}{\lambda_2}\left(V_{ref} - \beta V_o\right) + \beta V_o < \beta V_i$$

$$-K_{p1} i_c + K_{p2}\left(V_{ref} - \beta V_o\right) + \beta V_o = V_c$$

$$\hat{V}_{ramp} = \beta v_i$$

Where K_{P1} and K_{P2} are the constant gain parameters for the feedback signals i_c and ($V_{ref} - \beta V_0$). The values of K_{P1} and K_{P2} can be found in terms of converters parameters $L_{1,}$ $C_{1.}$

E .Parameters of the system

parameters	values
source	240 V
Output voltage	52V
Output current	151A
Switching frequency	35KHz
AC inductor (L3,L4)	2.5mH
Output capacitor(C1)	333uF
Input capacitor(C2)	14.8uF

F. Expected Results

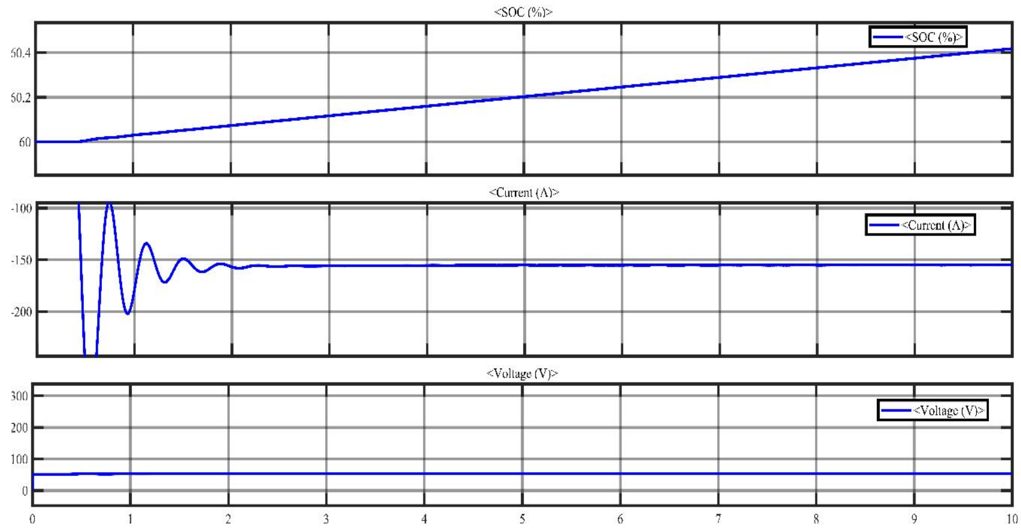

III. CONCLUSIONS

This paper proposes PWM-Based Sliding-Mode voltage controlled DC-DC converter for EV charging applications. The proposed converter's steady-state study demonstrates the relationship between input voltage, output voltage, and the prosecution in both ideal and non-ideal circumstances. For effective and economical operation, the DC and AC side inductors have been designed properly. The system may charge the lithium-ion battery with 152.1A while maintaining overshoot and other parameters with the suggested converter and prosecution. The suggested system will be more operationally, dependable and efficient by maintaining high power factor with low harmonic distortions.

REFERENCES

[1] M. R. Haque, S. Das, M. R. Uddin, M. S. I. Leon, and M. A. Razzak, ‘‘Performance evaluation of 1 kW asynchronous and synchronous buck converter-based solar-powered battery charging system for electric vehicles,’’ in Proc. IEEE Region Symp. (TENSYMP), Jun. 2020, pp. 770–773, doi:10.1109/TENSYMP50017.2020.9230833.

[2] M. R. Uddin, M. R. Uddin, K. F. I. Faruque, K. F. I. Faruque, P. Das, P. Das, K. M. Salim, and K. M. Salim, ‘‘An alternative PWM controlled high efficient solution for 60 V electric vehicle charging system to replace typical iron core charger: Technical performance assessment and comparison of efficiency,’’ in Proc. IEEE Region Symp. (TENSYMP), Jun. 2020, pp. 312–315, doi:10.1109/TENSYMP50017.2020.9231032.

[3] K. F. I. Faruque, M. R. Uddin, M. I. I. Sakib, and K. M. Salim, ‘‘Multiple outputs converter design for BMS integrated Li-ion battery charger appropriate for electric vehicle,’’ in Proc. Int. Conf. Sci. Contemp. Technol. (ICSCT), Aug. 2021, pp. 1–5, doi: 10.1109/ICSCT53883.2021.9642568.
[4] S. Das, K. M. Salim, and D. Chowdhury, ‘‘A novel variable width PWM switching based buck converter to control power factor correction phenomenon for an efficacious grid integrated electric vehicle battery charger,’’ in Proc. TENCON IEEE Region Conf., Nov. 2017, pp. 262–267, doi:10.1109/TENCON.2017.8227873.
[5] M. A. Razzak, S. B. Afzal, and M. M. Shabab, ‘‘A π-CLCL type immittance converter for constant current and dynamic load applications,’’ Int. J. Electr. Comput. Eng. (IJECE), vol. 4, no. 5, pp. 679–690, Oct. 2014, doi: 10.11591/ijece.v4i5.5957.
[6] R. N. Beres, X. Wang, F. Blaabjerg, M. Liserre, and C. L. Bak, ‘‘Optimal design of high-order passive-damped filters for grid-connected applications,’’ IEEE Trans. Power Electron., vol. 31, no. 4, pp. 2083–2098, Mar. 2016, doi: 10.1109/TPEL.2015.2441299.
[7] R. N. Beres, X. Wang, M. Liserre, F. Blaabjerg, and C. L. Bak, ‘‘A review of passive power filters for three-phase grid-connected voltage-source converters,’’ IEEE Trans. J. Emerg. Sel. Topics Power Electron., vol. 4, no. 1, pp. 54–69, Mar. 2016, doi: 10.1109/JESTPE.2015.2507203.
[8] M. Su, B. Cheng, Y. Sun, Z. Tang, B. Guo, Y. Yang, F. Blaabjerg, and H. Wang, ‘‘Single-sensor control of LCL-filtered grid-connected inverters,’’ IEEE Access, vol. 7, pp. 38481–38494, 2019, doi:10.1109/ACCESS.2019.2906239.
[9] M. R. Haque, S. Z. Eka, S. Ferdous, and M. A. Razzak, ‘‘Analysis of loss profile and thermal distribution of heat sink of IGBT-based asynchronous and synchronous buck converters for EV charging system,’’ in Proc. 5th Int. Conf. Electron., Mater. Eng. Nano-Technol. (IEMENTech), Sep. 2021, pp. 1–6, doi:10.1109/IEMENTech53263.2021.9614827.
[10] S. Chakraborty, M. M. Hasan, I. Worighi, O. Hegazy, and M. A. Razzak, ‘‘Performance evaluation of a PID-controlled synchronous buck converter based battery charging controller for solar-powered lighting system in a fishing trawler,’’ Energies, vol. 11, no. 10, p. 2722, Oct. 2018.
[11] M. R. Haque and M. A. Razzak, ‘‘A buck converter-based battery charging controller for electric vehicles using modified PI control system,’’ in Proc. IEEE Int. IoT, Electron. Mechatronics Conf. (IEMTRONICS), Apr. 2021, pp. 1–4, doi: 10.1109/IEMTRONICS52119.2021.9422646.
[12] M. R. Haque and S. Khan, ‘‘The modified proportional integral controller for the BLDC motor and electric vehicle,’’ in Proc. IEEE Int. IoT, Electron. Mechatronics Conf. (IEMTRONICS), Apr. 2021, pp. 1–5, doi: 10.1109/IEMTRONICS52119.2021.9422548.
[13] S. C. Tan, Y. M. Lai, C. K. Tse, and M. K. H. Cheung, “A fixedfrequency pulsewidth-modulation-based quasi-sliding-mode controller for buck converters,” IEEE Trans. Power Electron., vol. 20, no. 6, pp. 1379–1392, Nov. 2005.
[14] J. Mahdavi, M. R. Nasiri, A. Agah, and A. Emadi, “Application of neural networks and state-space averaging to a DC/DC PWM converter in sliding-mode operation,” IEEE/ASME Trans. Mechatron., vol. 10, no. 1, pp. 60–67, Feb. 2005.